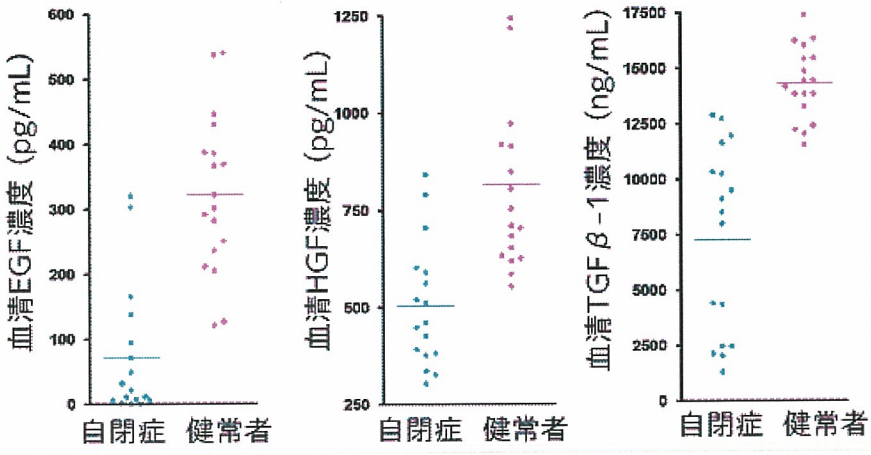

図1　高機能自閉症の血清学的異常（EGFの低下、HGFの低下、TGFβ1の低下）。これらが**診断指標となる可能性**が示唆された（Hashimoto et al., 2006; Shinohe et al., 2006; Suzuki et al., 2006）。

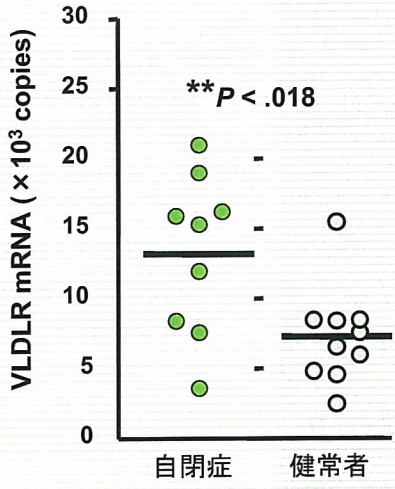

図2　高機能自閉症の末梢リンパ球における遺伝学的異常（リーリン受容体mRNAの増加）。リーリンは中枢神経の発生に重要な役割を果たす物質であることから、**リーリン受容体mRNAの発現は発症に関連する診断指標となる可能性**が示唆された（Nakamura et al., in preparation）。

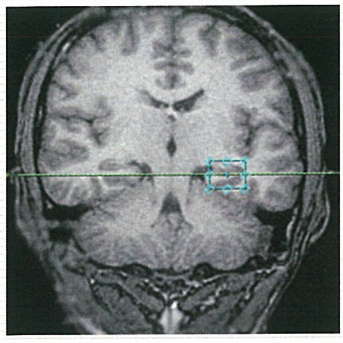

上記青色囲みは左海馬の関心領域を示す。

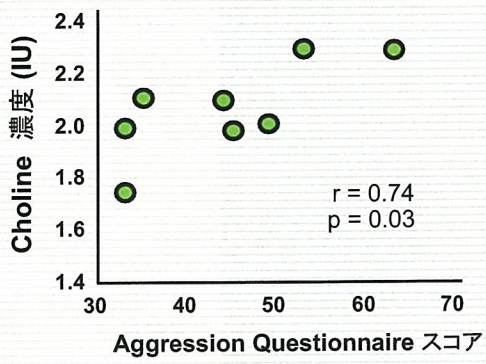

図3　高機能自閉症のMRS（脳磁気共鳴スペクトロスコピー）における左海馬のcholine濃度と、臨床的に評価された攻撃性の関連が示された。広汎性発達障害の**攻撃性が脳画像から予測されうる**ことが示唆された（Nakamura et al., in preparation）。

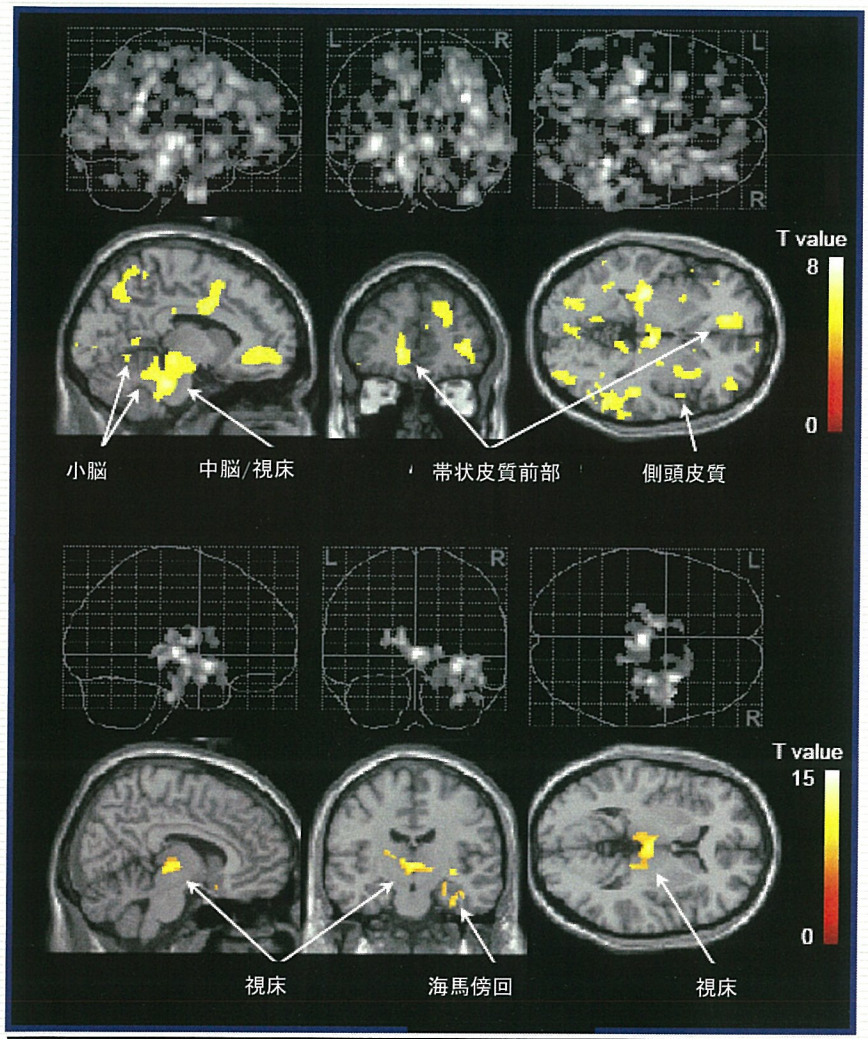

図4　PETを用いた高機能自閉症の脳では，黄色の脳部位でセロトニン・トランスポーター密度が低下していた（Nakamura et al., in preparation）。

図5　広汎性発達障害および自閉症の特徴的症状である「こだわり」（強迫症状）は，黄色の脳部位のセロトニン・トランスポーター密度の低下と関係していた（Nakamura et al., in preparation）。

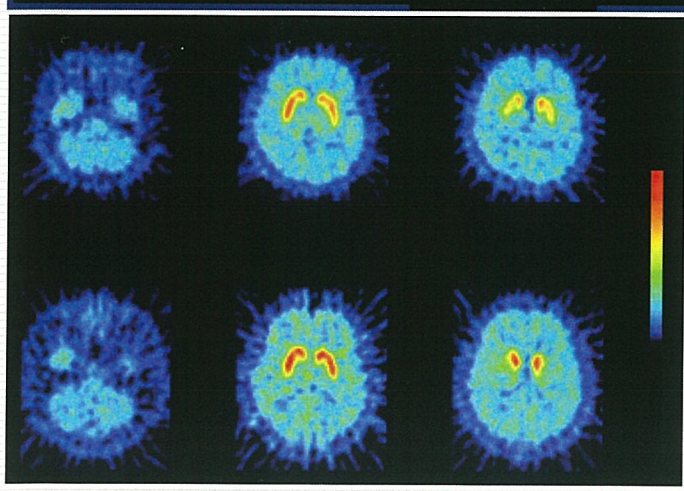

図6　高機能自閉症のドパミン・トランスポーター密度は、健常者と比較して高かった（Nakamura et al., in preparation）。

Ⅱ. 研究成果の刊行に関する一覧表

雑誌

発表者氏名	論文タイトル名	発表誌名	巻号	ページ	出版年
Yamamoto S, Ouchi Y, Onoe H, Yoshikawa E, Tsukada H, Takahashi H, Iwase M, Yamaguti K, Kuratsune H, Watanabe Y	Reduction of serotonin transporters of patients with chronic fatigue syndrome	Neuroreport	15	2571-2574	2004
Ouchi Y, Yoshikawa E, Kanno T, Futatsubashi M, Sekine Y, Okada H, Torizuka T, Tanaka K	Orthostatic posture affects brain hemodynamics and metabolism in cerebrovascular disease patients with and without coronary artery disease: a positron emission tomography study	Neuroimage	24	70-81	2004
Ouchi Y, Yoshikawa E, Sekine Y, Futatsubashi M, Kanno T, Ogusu T, Torizuka T	Microglial activation and dopamine terminal loss in early Parkinson's disease	Ann Neurol	57	168-175	2005
Takebayashi K, Sekine Y, Takei N, Minabe Y, Isoda H, Nishimura K, Nakamura K ,Suzuki K, Iwata Y, Sakahara H, Mori N	Metabolite alterations in basal ganglia associated with psychiatric symptoms of abstinent toluene users: a proton MRS study	Neuropsychopharmacology	29	1019-1026	2004
辻井正次、古橋由香	「アスペ・エルデの会」：当事者を主体とした高機能広汎性発達障害の地域発達支援システム	精神科	5	29-33	2004
辻井正次、竹嶋陽子	軽度発達障害をもつ子どもたちへの発達支援と治療教育：発達臨床心理学の視点から	学校保健研究	46	456-463	2004

浅井朋子、杉山登志郎、小石誠二、東　誠、並木典子、海野千畝子	軽度発達障害児が同朋に及ぼす影響の検討	Jpn. J. Child Adolesc.Psychiatr	45	360-371	2004
杉山登志郎、河邉眞千子	高機能広汎性発達障害青年の適応を決める要因	精神科治療学	19	1093-1100	2004
竹林和子・別府哲・宮本正一	教師は軽度発達障害児の問題行動をどのようにとらえているか－軽度発達障害についての理解と意識に関する質問紙調査	岐阜大学教育学部研究報告(人文科学)	53	239-248	2004
金子一史、本城秀次、村瀬聡美、野邑健二	母親から子どもへの愛着形成―心理社会的検討―	小児科臨床	57	1273-1279	2004
Sekine Y, Ouchi Y, Takei N, Yoshikawa E, Nakamura K, Futatsubashi M, Okada H, Minabe Y, Suzuki K, Iwata Y, Tsuchiya KJ, Tsukada H, Iyo M, Mori N.	Brain serotonin transporter density and aggression in abstinent methamphetamine abusers.	Arch Gen Psychiatry	63	90-100	2006
Tsuchiya K, Takagai S, Kawai M, Matsumoto H, Nakamura K, Minabe Y, Mori N, Takei N	Advanced paternal age associated with an elevated risk for schizophrenia in offspring in a Japanese population	Schizophr Res	76	337-342	2005
Ouchi Y, Kanno T, Yoshikawa E, Futatsubashi, Okada H, Torizuka T, Kaneko M.	Neural substrates in judgment process while playing go: a comparison of amateurs with professionals.	Cognitive Brain Reserach	23	164-170	2005

Ohmae E, Ouchi Y, Oda M, Suzuki T, Tobesawa S, Kanno T, Yoshikawa E, Futatsubashi M, Ueda Y, Okada H, Yamashita Y.	Cerebral hemodynamics evaluation by near-infrared time-resolved spectroscopy: Correlation with simultaneous positron emission tomography measurements	Neuroimage	29	697-705	2006
Kawai Y, Moriyama A, Asai K, Campbell CMC, Sumi S, Morishita H, Suchi M	Molecular characterization of histidinemia:identification of four missense mutations in the hisitidase gene	Hum Genet	116	340-346	2005
Sumi S, Taniai H, Miyachi T, Tanemura M	Sibling risk of pervasive developmental disorder estimated by means of an epidemiologic survey in Nagoya, Japan.	J Hum Genet	51	518-522	2006
杉山登志郎	自閉症臨床から	小児の精神と神経	45	336-362	2005
浅井朋子、杉山登志郎、小石誠二、東　誠、遠藤太郎、大河内修、海野千畝子、並木典子、河邊真千子、服部麻子	高機能広汎性発達障害の母子例への対応	小児の精神と神経	45	313-321	2005
別府哲・野村香代	高機能自閉症児は健常児と異なる「心の理論」をもつのか：「誤った信念」課題とその言語的理由付けにおける健常児との比較	発達心理学研究	16	257-264	2005
鷲見　聡、宮地泰士、谷合弘子、石川道子	名古屋市西部における広汎性発達障害の有病率－療育センター受診児数からの推定値－	小児の精神と神経	46	57-60	2006
並木典子、杉山登志郎、明翫光宣	高機能広汎性発達障害にみられる気分障害に関する臨床的研究	小児の精神と神経	46	257-263	2006
杉山登志郎	アスペルガー症候群の現状	日本臨床	65	401-406	2007
別府哲	自閉症児の他者理解の発達における機能連関の特異性～愛着，共同注意，誤った信念課題	自閉症スペクトラム研究	5	1-8	2006

別府哲	自閉症における他者理解の機能連関と形成プロセスの特異性	障害者問題研究、	34	19-26	2007
鷲見　聡	自閉症スペクトラムの原因について　―多因子疾患説を中心に―	小児科臨床	60	127-134	2007
辻井正次、桜井伸二、佐竹創平	広汎性発達障害の３次元動作分析からみた投動作のバリエーション	中京大学社会学部紀要	21	41-54	2007
辻井正次、行廣隆次、安達　潤、市川宏伸、井上雅彦、内山登紀夫、神尾陽子、栗田広、杉山登志郎	日本自閉症協会広汎性発達障害評価尺度（PARS）幼児期尺度の信頼性・妥当性の検討	臨床精神医学	35	1119-1126	2006
安達　潤、行廣隆次、井上雅彦、内山登紀夫、神尾陽子、栗田広、杉山登志郎、辻井正次、市川宏伸	日本自閉症協会広汎性発達障害評価尺度（PARS）児童尺度の信頼性・妥当性の検討	臨床精神医学	35	1591-1599	2006
神尾陽子、行廣隆次、安達　潤、市川宏伸、井上雅彦、内山登紀夫、栗田広、杉山登志郎、辻井正次	思春期から成人期における広汎性発達障害の行動チェックリスト日本自閉症協会広汎性発達障害評価尺度（PARS）の信頼性・妥当性についての検討	精神医学	48	495-505	2006
Shinohe A, Hashimoto K, Nakamura K, Tsujii M, Iwata Y, Tsuchiya K, Sekine Y, Takai Y, Suzuki K, Sugihara G, Minabe Y, Ouchi Y, Sugiyama T, Iyo M, Takei N, Mori N	Increased serum levels of glutamate in adult patients with autism	Prog Neuropsychopharmacol Biol Psychiatry.	30	1472-7	2006
Hashimoto K, Iwata Y, Nakamura K, Tsujii M, Tsuchiya KJ, Sekine Y, Suzuki K, Minabe Y, Takei N, Iyo M, Mori N.	Reduced serum levels of brain-derived neurotrophic factor in adult male patients with autism.	Prog Neuropsychopharmacol Biol Psychiatry.	30	1529-31	2006

Okada K, Hashimoto K, Iwata Y, Nakamura K, Tsujii M, Tsuchiya KJ, Sekine Y, Suda S, Suzuki K, Sugihara GI, Matsuzaki H, Sugiyama T, Kawai M, Minabe Y, Takei N, Mori N.	Decreased serum levels of transforming growth factor-betal in patients with autism.	Prog Neuropsychop harmacol Biol Psychiatry.	30	187-90.	2007
Suzuki K, Hashimoto K, Iwata Y, Nakamura K, Tsujii M, Tsuchiya K, Sekine Y, Suda S, Sugihara G, Matsuzaki H, Sugiyama T, Kawai M, Minabe Y, Takei N, Mori N.	Decreased Serum Levels of Epidermal Growth Factor in Adult Subjects with High-Functioning Autism.	Biological Psychiatry.	356		2006 in press
Sugihara G, Hashimoto K, Iwata Y, Nakamura K, Tsujii M, Tsuchiya KJ, Sekine Y, Suzuki K, Suda S, Matsuzaki H, Kawai M, Minabe Y, Yagi A, Takei N, Sugiyama T, Mori N.	Decreased serum levels of hepatocyte growth factor in male adults with high-functioning autism.	Prog Neuropsychop harmacol Biol Psychiatry.	31	412-5	2007
Nishimura K, Nakamura K, Anitha A, Yamada K, Tsujii M, Iwayama Y, Hattori E, Toyota T, Takei N, Miyachi T, Iwata Y, Suzuki K, Matsuzaki H, Kawai M, Sekine Y, Tsuchiya K, Sugihara G, Suda S, Ouchi Y, Sugiyama T, Yoshikawa T, Mori N.	Genetic analyses of the brain-derived neurotrophic factor (BDNF) gene in autism.	Biochem Biophys Res Commun.	356	200-6.	2007

Tsuchiya KJ, Hashimoto K, Iwata Y, Tsujii M, Sekine Y, Sugihara G, Matsuzaki H, Suda S, Kawai M, Nakamura K, Minabe Y, Yagi A, Iyo M, Takei N, Mori N.	Decreased serum levels of PECAM-1 in subjects with high-functioning autism: a negative correlation with head circumference at birth.	Biol Psychiatry			2007 in press.
Sadakata T, Washida M, Iwayama Y, Shoji S, Sato Y, Ohkura T, Katoh-Semba R, Nakajima M, Sekine Y, Tanaka M, Nakamura K, Iwata Y, Tsuchiya KJ, Mori N, Detera-Wadleigh SD, Ichikawa H, Itohara S, Yoshikawa T, Furuichi T.	Autistic-like phenotypes in Cadps2-knockout mice and aberrant CADPS2 splicing in autistic patients.	J Clin Invest.	17	931-43	2007

Reduction of serotonin transporters of patients with chronic fatigue syndrome

Shigeyuki Yamamoto, Yasuomi Ouchi,[1] Hirotaka Onoe,[2] Etsuji Yoshikawa,[3] Hideo Tsukada,[3] Hidetoshi Takahashi,[4] Masao Iwase,[4] Kouzi Yamaguti,[5] Hirohiko Kuratsune[5,6] and Yasuyoshi Watanabe[CA]

Department of Physiology, Osaka City University Graduate School of Medicine, 1-4-3 Asahimachi, Abeno-ku, Osaka 545-8585; [1]Positron Medical Center, Hamamatsu Medical Center, 5000 Hirakuchi, Hamakita, Shizuoka 434-0041; [2]Department of Psychology, Tokyo Metropolitan Institute for Neuroscience, 2-6 Musashidai Fuchu, Tokyo 183-8526; [3]Central Research Laboratory, Hamamatsu Photonics KK, 5000 Hirakuchi, Hamakita, Shizuoka 434-8601; [4]Psychiatry, Department of Clinical Neuroscience; [5]Department of Hematology and Oncology, Osaka University Graduate School of Medicine, 2-2 Yamadaoka, Suita 565-0871; [6]Department of Health Sciences, Faculty of Health Sciences for Welfare, Kansai University of Welfare Sciences, 3-11-1 Asahigaoka, Kashiwara 582-0026, Japan

[CA]Corresponding Author: yywata@med.osaka-cu.ac.jp

Received 10 September 2004; accepted 6 October 2004

To assess the involvement of serotonin in the symptoms of chronic fatigue syndrome, we investigated the serotonergic neurotransmitter system of chronic fatigue syndrome patients by the positron emission tomography (PET). Here we show that the density of serotonin transporters (5-HTTs) in the brain, as determined by using a radiotracer, [^{11}C](+)McN5652, was significantly reduced in the rostral subdivision of the anterior cingulate as compared with that in normal volunteers. This subdivision is different from that in the dorsal anterior cingulate in which binding potential values of individual patient showed a weak negative correlation with self-reported pain score of the patients. Therefore, an alteration of serotonergic system in the rostral anterior cingulate plays a key role in pathophysiology of chronic fatigue syndrome. *NeuroReport* 15:2571–2574 © 2004 Lippincott Williams & Wilkins.

Key words: Anterior cingulate; Chronic fatigue syndrome; Fatigue; Positron emission tomography (PET); Serotonin transporter

INTRODUCTION

Chronic fatigue syndrome is a disorder characterized by profound disabling fatigue that persists for at least 6 months without relief, being unsatisfied by ordinary rest [1]. Musculoskeletal pain or nonpsychotic depression often accompanies chronic fatigue syndrome. Although no effective somatic treatment for chronic fatigue syndrome has been established yet, selective serotonin reuptake inhibitors (SSRIs) have often been prescribed and have been reported to be effective in non-depressed patients as well as or better than in depressed patients though this effect was not confirmed when one of SSRIs, fluoxetine, was tried [2]. Our recent treatment study with fluvoxamine demonstrated the improvement in 36% of patients [3]. Serotonergic abnormalities have also been reported from endocrinological studies that showed a high sensitivity of serotonin (5-HT) neurotransmission in chronic fatigue syndrome patients [4,5]. In addition, a study on polymorphism of the promoter region of the 5-HT transporter (5-HTT) gene revealed a difference in genotype distribution between chronic fatigue syndrome patients and controls [6]. The role of the serotonergic system in chronic pain has been highlighted [7], especially, in the patients with fibromyalgia, a disease closely related to chronic fatigue syndrome in which pain is more centered than in chronic fatigue syndrome.

A PET study with [^{18}F]-FDG PET reported that chronic fatigue syndrome patients showed a significant hypometabolism in right mediofrontal cortex and brain stem in comparison with the healthy controls [8]. Siessmeier *et al.* [9] also demonstrated by PET that 12 of 26 patients examined showed hypometabolism bilaterally in the cingulate gyrus and the adjacent mesial cortical areas. Our previous PET studies on patients showed that hypoperfusion and decrease in uptake of the acetyl moiety of acetyl-L-carnitine as measured with [2-^{11}C]acetyl-L-carnitine (an indicator of glutamate biosynthesis) occurred in several regions of the brains of the patient group, namely, in the prefrontal (Brodmann's area 9/46d) and temporal (Brodmann's area 21 and 41) cortices, anterior cingulate (Brodmann's area 24 and 33), and cerebellum [10].

These lines of evidence led us to investigate the 5-HT neurotransmission in the brain of chronic fatigue syndrome patients. Here, we measured the density of 5-HTTs by using PET with [^{11}C](+)McN5652, which binds specifically to the 5-HTT molecule and is widely used to study 5-HTTs in the brains of Ecstasy abusers [11] and patients with obsessive-compulsive disorder [12].

MATERIALS AND METHODS

Subjects: Ten patients with chronic fatigue syndrome (six women and four men, 35.7±8.0 years old) determined by the clinical diagnostic criteria [1] and 10 age-matched healthy controls (five women and five men, 36.9±10.1 years old) participated in this study. Patients with a major depressive disorder determined by diagnostic and statistical manual (DSM-IV) of mental disorders and taking drugs affecting 5-HT neurons within 1 month before the start of the study were excluded. Eight of the patients were naive for SSRIs; and the other two, who had been prescribed

paroxetine, had not been medicated within 1 month before the experimental day. The study was approved by the Ethics Committee of Hamamatsu Medical Center. All participants agreed to the present study with their written informed consent. Patients filled out a questionnaire about their extent of fatigue [expressed by the visual analogue scale], pain scales of headache, sore throat, myalgia, and arthralgia (pain scale: 0, none; 1, mild; 2, moderate; and 3, severe), attention score calculated by thinking difficulty, inability to concentration, impairment in memory, and absence of alertness (each scale: 0, none; 1, mild; 2, moderate; and 3, severe), and duration of disease. The total sum of the pain scale values and attention scores with four items was used as the pain and attention score for each group, respectively. Depression scale was assessed using the 17-item Hamilton Depression Rating Scale (HDRS-17) [13].

MRI and PET experiments: MRI acquired by a 0.3 T scanner (MRP7000AD, Hitachi, Tokyo, Japan) of each subject revealed no apparent morphological abnormalities. The specific radioactivity ranged from 46.6 to 88.2 GBq/μmol. After a bolus injection of [^{11}C](+)McN5652 (390.7±71.9 MBq), PET scan was performed with a duration of 92 min (4 × 30 s, 20 × 1 min, and 14 × 5 min), using a SHR12000 (Hamamatsu Photonics KK, Hamamatsu, Japan) scanner in 3D.

PET data analysis: We generated parametric images of the binding potential (BP) by a simplified reference tissue model based on pixel-wise kinetic modelling [14] using a time-activity curve of bilateral white matter as an input function. We normalized the images spatially within the standard Montreal Neurological Institute (MNI) brain space by using SPM99. The resultant images were smoothed using a Gaussian filter of 8.0 mm FWHM. We performed two-tailed *t*-tests between patients and controls, and conducted correlation analysis between the BP value and the clinical symptomatic scores of the patients. We gave the threshold of significance as voxels that had the peak height corrected, $p<0.05$ for the two-tailed *t*-tests. For the correlation analysis, we also searched the brain regions which shows tendency of significance by a threshold of $p<0.001$.

RESULTS

As shown in Table 1, fatigue scores, as indexed by visual analogue scale, were in a narrow range both in patients and controls (7.3±1.6 *vs* 2.7±1.0, respectively). In contrast, the pain scores for the chronic fatigue syndrome group were scattered (from 2 to 11, 5.8±3.0), and those for the controls were almost 0 or 1 (0.3±0.5). The attention score showing less attentive feature was 6.7±1.7 and 2.5±2.5 in the patients and controls, respectively. Fatigue, pain, and attention scores were significantly higher for the chronic fatigue syndrome patients than for the controls ($p<0.0001$, $p<0.0005$, and $p<0.0005$, respectively). The depression score (HDRS-17) was ranged from 5 to 22 in the patient group (11.5±5.3). Although the score was rather high in chronic fatigue syndrome patients, the main source of higher scores was derived mostly from higher scores on work and activities, and the somatic items such as somatic symptoms general, anxiety somatic, and hypochondriasis (date not shown). However, there were no significant correlation among visual analogue scale and other three clinical scores (pain, attention, and depression).

The PET results of the two-tailed *t*-test showed a significant reduction of the BP in the rostral subdivision of anterior cingulate (BA24/32) in chronic fatigue syndrome patients (Fig. 1a–c). The BP in the rostral anterior cingulate was decreased by 26.5% in the chronic fatigue syndrome patients, with its mean values for controls and patients being 0.82±0.04 and 0.61±0.08, respectively (Fig. 1d).

Correlation analysis using various clinical scores in chronic fatigue syndrome patients showed that no correlation was significant at the corrected level of $p<0.05$. If the tendency was followed by lowering the statistical threshold to uncorrected $p<0.001$, pain score showed a negative correlation with the BP in anterior cingulate (Fig. 2a,c) and other areas related to pain sensation, including cuneus/precuneus (BA18, Z=4.8), orbitofrontal cortex (BA11/47, Z=3.76), posterior cingulate (BA31, Z=3.64), and insular cortex, Z=3.32; Fig. 2a,b). The locus in the anterior cingulate was however in the dorsal subdivision (Fig. 2a,b), an apparently different region from the rostral subdivision. All the other scores and values of clinical symptoms such as depression, attention, and duration of disease showed no

Table 1. Summary of demographic data in 10 patients with chronic fatigue syndrome (CFS) and normal controls.

Group	Patient no.	Age	Sex	EP	DD	Comorbidity	Antidepressant	HDRS-17	VAS	Attention score[2]	Pain score[3]
CFS	1	45	M	18	6	CD	–	5	6.1	8	3
	2	46	M	16	5	None	+[1]	17	7.8	8	8
	3	30	M	12	3	None	–	7	9.6	7	3
	4	27	M	16	3	None	–	13	6.4	6	5
	5	46	F	16	15	usd	–	9	6.4	8	10
	6	27	F	16	8	usd	–	14	9	3	4
	7	37	F	14	0.5	None	–	9	4.8	5	2
	8	27	F	12	13	usd	+[1]	22	5.6	8	11
	9	39	F	16	11	None	–	13	7.8	8	6
	10	33	F	18	4	None	–	6	9.1	6	6
	Mean	35.7		15.4	6.9			11.5	7.3	6.7	5.8
	SD	8		2.1	4.8			5.3	1.6	1.7	3
Normal	Mean	36.9	5M	15.6					2.7	2.5	0.3
	SD	10.1	5F	2.1					1	2.5	0.5

EP, education period (years); DD, disease duration (years); HDRS-17, the 17-item hamilton depression rating scale; VAS, visual analogue scale; CD, conversion disorder; usd, undifferentiated somatoform disorder.

[1]Patient no.2 was medicated by SSRIs, fluvoxamine and paroxetine for 12 months and 15 months, respectively. Patient no. 8 was medicated by paroxetine for 13 months.

[2]Thinking difficulty, inability to concentrate, impairment in memory, and absence of alertness scales (0, none; 1, mild; 2, moderate; and 3, severe) were summed up as the attention score.

[3]Headache, sore throat, myalgia, and arthralgia scales (0, none; 1, mild; 2, moderate; and 3, severe) were summed up as the pain score.

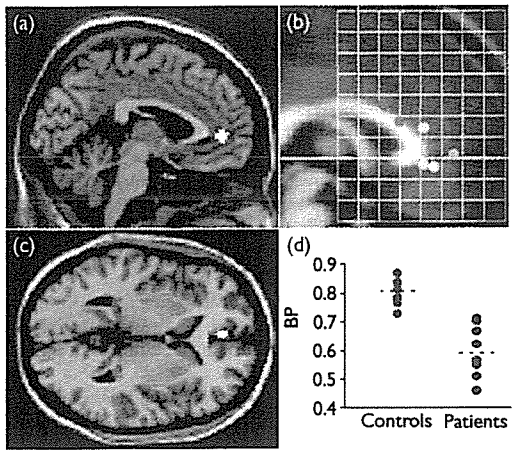

Fig. 1. The region showing a significant reduction in the BP of 5-HTT in chronic fatigue syndrome patients. (**a**) Sagittal and (**b**) horizontal views of statistical parametric maps superimposed on a normalized brain MRI. BP of the rostral subdivision of anterior cingulate (BA24/32) was significantly reduced (corrected p=0.008, Z=4.95) in chronic fatigue syndrome patients. The cluster consisted of 39 voxels extending from the MNI brain space coordinates (x −2, y 46, z 2). (**c**) The coordinates of the cluster observed in the present study (green circle) is compared with those of previous PET studies demonstrating a reduction in the rCBF shown by blue circles [10], regional standard uptake value of [2-^{11}C]acetyl-L-carnitine shown by purple circles [10], and regional glucose metabolism shown by a yellow circle [9]. (**d**) Plots of BP in the rostral anterior cingulate of controls and chronic fatigue syndrome patients.

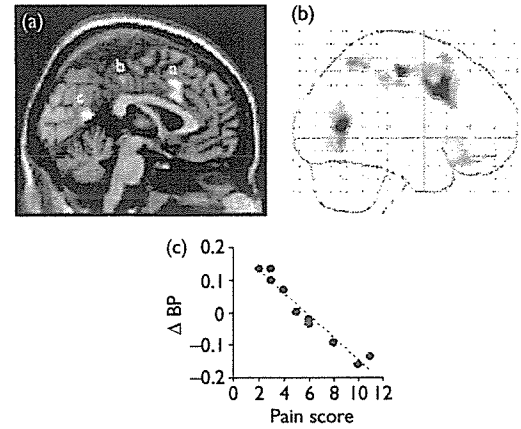

Fig. 2. The region showing a negative correlation between the BP of 5-HTT and the pain score. (**a**) Sagittal view of statistical parametric maps superimposed on a normalized brain MRI, and (**b**) sagittal view of standard SPM-glass brain. BP in the dorsal subdivision of anterior cingulate (BA24) was negatively correlated (uncorrected $p<0.0001$, Z=4.71) with the pain score. The cluster consisted of 1058 voxels extending from the MNI brain space coordinates (x 4, y 16, z 42). (a) Dorsal anterior cingulate (BA24/32); (b) posterior cingulate cortex (BA31); (**c**) cuneus/precuneus (BA18). (**c**) Scatter plots showing the negative correlation between the BP and the pain score in the dorsal anterior cingulate.

significant correlation at any brain regions including anterior cingulate, even under lowered statistical threshold.

DISCUSSION

Alteration of 5-HTT density occurred selectively in the rostral subdivision of anterior cingulate in patients with chronic fatigue syndrome. Previous histological examination showed dense serotonergic projections from the dorsal raphe nucleus to the anterior cingulate [15]. Lower than normal 5-HTT density was also detected by single-photon emission-computed tomography (SPECT) in the brain of patients with major depression [16] and in postmortem studies [17,18], mostly related to the suicide; but the affected regions were dominantly the prefrontal cortex and midbrain including the dorsal raphe nucleus. The reduction of 5-HTT specifically in the discrete region of anterior cingulate might be linked to the pathophysiology of non-depressed chronic fatigue syndrome patients in this study.

BP (k3/k4) of [^{11}C](+)McN5652 calculated by compartment model is considered to be related with the B_{max}/K_d to the 5-HTT molecule. Therefore, reduction of BP observed in the anterior cingulate might be associated with decrement of density of 5-HTT and/or affinity. A possible interpretation of the data is that the reduction in BP is due to the increase in 5-HT in the synaptic cleft, as shown in the case of [^{11}C]raclopride for increase in endogenous dopamine release [19]. In a study of Ecstasy abusers, McCann *et al.* [11] reported the reduction of density of 5-HTT in the nerve terminals. The other interpretation is the degeneration of the nerve terminals themselves. To solve this question, the PET study using [^{11}C]5-HTP in chronic fatigue syndrome patients is currently under progress in our laboratory.

Concerning expression of 5-HTT in diseases, even in the case of major depressive disorder, the results from the PET imaging studies and those from the biochemical studies on postmortem brain tissues from patients [20], mostly suicidal ones, are still controversial. Recently, our colleagues [6] found a difference between chronic fatigue syndrome patients and controls in the distribution of polymorphism of the 5-HTT gene promoter. Association between polymorphism of the 5-HTT gene promoter and the expression of 5-HTT protein in the brain is unclear yet [21]. It is of very importance to further study on the association between genotype and phenotype in chronic fatigue syndrome patients.

The anterior cingulate consists of functionally heterogeneous regions, and the rostral subdivision is thought to be involved in the processing of emotional information [22]. The rostral anterior cingulate, in which BP values of 5-HTT were significantly reduced in chronic fatigue syndrome patients, is distinct from the dorsal anterior cingulate associated with the cognitive information processing. Comorbidities of chronic fatigue syndrome which are closely related to emotional aspects might be associated with the loss of modulatory function of 5-HT released possibly from 5-HT nerve-terminals in the rostral subdivision. The locus in the dorsal subdivision that was not significantly but by lower threshold correlated negatively with the pain score of chronic fatigue syndrome patients is close to the locus of pain processing found in the previous PET studies [23,24]. Concerning other brain regions, although none of the brain regions reached to the statistically significant level at $p<0.05$ (corrected), most of the regions negatively correlated with the pain score at lower threshold ($p<0.001$, uncorrected; Fig. 2) were consistent with those which were suggested to be involved in several aspects of pain information processing by recent fMRI and PET experiments [24], indicating the role of 5-HT neurotransmission of these regions in pain-related features of chronic fatigue syndrome patients. Therefore, reduced 5-HTT in the rostral anterior cingulate of the chronic fatigue syndrome patients might be related to the pathogenesis of the disease, not to the non-specific symptom of pain, although we should be careful about the discrimination of

chronic fatigue syndrome patients from the patients who are suffering mostly with stronger pain, fibromyalgia.

Figure 1c shows loci of anterior cingulate observed in this study and previous PET studies on chronic fatigue syndrome. These loci associated with chronic fatigue syndrome totally converged in the anterior cingulate. Apart from the dorsal subdivision, the hypoactivity, hypometabolism, and dysfunction of 5-HT neurotransmission concomitantly occurred in the rostral subdivision. Therefore, these findings strongly suggest that an abnormality of 5-HT neurotransmission, especially the reduction in the density of presynaptic terminals of the serotonergic system in the projection area of the anterior cingulate, might be closely associated with the pathophysiology of chronic fatigue syndrome.

Although regional cerebral blood flow (rCBF) of chronic fatigue syndrome patients was not measured in the present study, the decreased BP value of 5-HTT may be partly affected by the hypoperfusion in anterior cingulate reported in the previous PET study [10]. However, decreases in rCBF were also significant in several regions such as middle occipital gyrus, putamen, insula, and so on, while a significant decrease in BP value of 5-HTT in the present study was only observed in the rostral part of anterior cingulate. Therefore, the decrease in BP value might be more likely due to the decrease in density and/or affinity of 5-HTT.

As described in the Introduction, the results of clinical treatment of chronic fatigue syndrome patients with SSRIs are still controversial. Several detrimental effects, such as nausea, headache, and nervousness often disturb and mask the beneficial effects of SSRIs at the beginning of a clinical trial. In addition, increment of risk of suicide by use of SSRIs has been issued recently as a considerable public warning, especially in teenager patients. Therefore, quantitative PET imaging analysis for measuring the brain 5-HTT density with a specific radiotracer, such as [^{11}C]McN5652 used in this study, is feasible for both judging and monitoring the medication of individual chronic fatigue syndrome patients.

CONCLUSION

The density of 5-HTTs was significantly reduced in the rostral subdivision of anterior cingulate in chronic fatigue syndrome patients. An alteration of the 5-HTergic system in the rostral anterior cingulate plays a key role in pathophysiology of the chronic fatigue syndrome.

REFERENCES

1. Fukuda K, Straus SE, Hickie I, Sharpe MC, Dobbins JG and Komaroff A. The chronic fatigue syndrome: a comprehensive approach to its definition and study. International Chronic Fatigue Syndrome Study Group. *Ann Intern Med* 1994; **121**:953–959.
2. Vercoulen JH, Swanink CM, Zitman FG, Vreden SG, Hoofs MP, Fennis JF *et al.* Randomised, double-blind, placebo-controlled study of fluoxetine in chronic fatigue syndrome. *Lancet* 1996; **347**:858–861.
3. Kuratsune H. The current treatment for patients with chronic fatigue syndrome: fluvoxamine, amantadine and herbal medicine. *J Chronic Fatigue Syndr*, in press.
4. Bakheit AM, Behan PO, Dinan TG, Gray CE and O'Keane V. Possible upregulation of hypothalamic 5-hydroxytryptamine receptors in patients with postviral fatigue syndrome. *Br Med J* 1992; **304**:1010–1012.
5. Cleare AJ, Bearn J, Allain T, McGregor A, Wessely S, Murray RM *et al.* Contrasting neuroendocrine responses in depression and chronic fatigue syndrome. *J Affect Disord* 1995; **35**:283–289.
6. Narita M, Nishigami N, Narita N, Yamaguti K, Okado N, Watanabe Y *et al.* Association between serotonin transporter gene polymorphism and chronic fatigue syndrome. *Biochem Biophys Res Commun* 2003; **311**:264–266.
7. Grothe DR, Scheckener B and Albano D. Treatment of pain syndromes with venlafaxine. *Pharmacotherapy* 2004; **24**:621–629.
8. Tirelli U, Chierichetti F, Tavio M, Simonelli C, Bianchin G, Zanco P *et al.* Brain positron emission tomography (PET) in chronic fatigue syndrome: preliminary data. *Am J Med* 1998; **105**:54S–58S.
9. Siessmeier T, Nix WA, Hardt J, Schreckenberger M, Egle UT and Bartenstein P. Observer independent analysis of cerebral glucose metabolism in patients with chronic fatigue syndrome. *J Neurol Neurosurg Psych* 2003; **74**:922–928.
10. Kuratsune H, Yamaguti K, Lindh G, Evengård B, Hagberg G, Matsumura K *et al.* Brain regions involved in fatigue sensation: reduced acetylcarnitine uptake into the brain. *Neuroimage* 2002; **17**:1256–1265.
11. McCann UD, Szabo Z, Scheffel U, Dannals RF and Ricaurte GA. Positron emission tomographic evidence of toxic effect of MDMA ("Ecstasy") on brain serotonin neurons in human beings. *Lancet* 1998; **352**:1433–1437.
12. Simpson HB, Lombardo I, Slifstein M, Huang HY, Hwang DR, Abi-Dargham A *et al.* Serotonin transporters in obsessive-compulsive disorder: a positron emission tomography study with [^{11}C]McN 5652. *Biol Psychiatry* 2003; **54**:1414–1421.
13. Williams JB. A structured interview guide for the Hamilton Depression Rating Scale. *Arch Gen Psychiatry* 1988; **45**:742–747.
14. Buck A, Gucker PM, Schönbächler RD, Arigoni M, Kneifel S, Vollenweider FX *et al.* Evaluation of serotonergic transporters using PET and [^{11}C](+)McN-5652: assessment of methods. *J Cerebr Blood Flow Metab* 2000; **20**:253–262.
15. Wilson MA and Molliver ME. The organization of serotonergic projections to cerebral cortex in primates: regional distribution of axon terminals. *Neuroscience* 1991; **44**:537–553.
16. Malison RT, Price LH, Berman R, van Dyck CH, Pelton GH, Carpenter L *et al.* Reduced brain serotonin transporter availability in major depression as measured by [^{123}I]2 beta-carbomethoxy-3 beta-(4-iodophenyl)tropane and single photon emission computed tomography. *Biol Psychiatry* 1998; **44**:1090–1098.
17. Arango V, Underwood MD, Gubbi AV and Mann JJ. Localized alterations in pre- and postsynaptic serotonin binding sites in the ventrolateral prefrontal cortex of suicide victims. *Brain Res* 1995; **7**:121–133.
18. Mann JJ, Huang YY, Underwood MD, Kassir SA, Oppenheim S, Kelly TM *et al.* A serotonin transporter gene promoter polymorphism (5-HTTLPR) and prefrontal cortical binding in major depression and suicide. *Arch Gen Psychiatry* 2000; **57**:729–738.
19. M. Imaging synaptic neurotransmission with *in vivo* binding competition techniques: a critical review. *J Cerebr Blood Flow Metab* 2000; **20**:423–51.
20. Stockmeier CA. Involvement of serotonin in depression: evidence from post-mortem and imaging studies of serotonin receptors and the serotonin transporter. *J Psych Res* 2003; **37**:357–373.
21. Collier DA, Stober G, Li T, Heils A, Catalano M, Di Bella D *et al.* A novel functional polymorphism within the promoter of the serotonin transporter gene: possible role in susceptibility to affective disorders. *Mol Psychiatry* 1996; **1**:453–460.
22. Shioe K, Ichimiya T, Suhara T, Takano A, Sudo Y, Yasuno F *et al.* No association between genotype of the promoter region of serotonin transporter gene and serotonin transporter binding in human brain measured by PET. *Synapse* 2003; **48**:184–188.
23. Bush G, Luu P and Posner MI. Cognitive and emotional influences in anterior cingulate cortex. *Trends Cogn Sci* 2000; **4**:215–222.
24. Rainville P, Duncan GH, Price DD, Carrier B and Bushnell MC. Pain affect encoded in human anterior cingulate but not somatosensory cortex. *Science* 1997; **277**:968–971.
25. Peyron R, Laurent B and Garcia-Larrea L. Functional imaging of brain responses to pain. A review and meta-analysis (2000). *Neurophysiol Clin* 2000; **30**:263–288.

Acknowledgements: This study was performed through Special Coordination Funds for Promoting Science and Technology from the Ministry of Education, Culture, Sports, Science and Technology of the Japanese Government.

ELSEVIER

NeuroImage

www.elsevier.com/locate/ynimg
NeuroImage 24 (2005) 70–81

Orthostatic posture affects brain hemodynamics and metabolism in cerebrovascular disease patients with and without coronary artery disease: a positron emission tomography study

Yasuomi Ouchi,[a,b,*] Etsuji Yoshikawa,[c] Toshihiko Kanno,[a] Masami Futatsubashi,[c] Yoshimoto Sekine,[a,c] Hiroyuki Okada,[c] Tatsuo Torizuka,[a] and Keisei Tanaka[d]

[a]*Positron Medical Center, Hamamatsu Medical Center, Hamakita, Japan*
[b]*Department of Neurology, Hamamatsu Medical Center, Hamamatsu, Japan*
[c]*Central Research Laboratory, Hamamatsu Photonics K.K., Hamakita, Japan*
[d]*Department of Neurosurgery, Hamamatsu Medical Center, Hamamatsu, Japan*

Received 27 January 2004; revised 8 July 2004; accepted 12 July 2004

To investigate whether a physiological change in the orthostatic condition is associated with a deterioration of cerebrovascular and metabolic homeostasis in patients with neurocardiovascular compromises, we examined 10 patients with unilateral carotid artery occlusive disease (CVD), 6 CVD patients with coronary artery disease (CVDC), and 10 healthy subjects scanned twice under supine and sitting conditions by positron emission tomography (PET). Repeated measures analysis of variance showed significant reductions in regional cerebral blood flow (rCBF) and cerebral oxygen metabolism ($rCMRO_2$) and tendency of increase in oxygen extraction fraction (OEF) in the affected-side parietal cortex during assuming of upright posture in the CVDC group, and there was a significant OEF increase to maintain $rCMRO_2$ constant during sitting in the CVD counterpart. In this ischemic region, there were negative correlations between changes in OEF and rCBF in the CVD ($P < 0.05$) and CVDC groups ($P < 0.01$). Postural reductions in rCBF and CMRO2 in the parietal region were significantly greater in the CVDC group than those in the CVD group. While rCBF remained constant with mean arterial blood pressure (MABP) in healthy subjects, an rCBF reduction was found in the affected parietal cortex in proportion to the upright posture-induced MABP decrease in the CVDC group. These results indicate that patients suffering from both cerebral and coronary artery diseases may be at greater risk of deterioration of local perfusion pressure and metabolic regulation in the hemodynamically susceptible brain region during upright posture.

Keywords: Cerebral artery occlusion; Upright posture; Cerebral oxygen metabolism; Cerebral blood flow; Positron emission tomography

Introduction

It is widely accepted that a sudden reduction in blood pressure can affect cerebral blood flow (CBF) and render an elderly subject vulnerable to orthostatic symptoms such as dizziness, falls, or syncope (Graafmans et al., 1996; Lipsitz, 1989). A prolonged upright posture could trigger syncope even in healthy subjects, due chiefly to neurally mediated (vasovagal) fainting (Kapoor, 2000), and in patients with coronary artery disease, due to impairments in blood pressure regulation (Pitzalis et al., 2002). Therapeutically, it has been reported that in healthy subjects, drinking a substantial amount of water helps prevent deterioration of CBF regulation during the head-up tilt condition (Schroeder et al., 2002). These findings suggest that an orthostatic physiological change during head-up posture would be more dangerous to stroke patients, because their ischemic brain regions are likely susceptible to local hypoperfusion changes during sitting (Ouchi et al., 2001a). Thus, it is expected that not only CBF, but also metabolic regulation, would vary dynamically while human subjects are in an upright posture, especially those patients with hemodynamically compromised cerebrocardiovascular circulation, for example, major cerebral artery occlusion with coronary artery stenosis.

Many investigators have so far reported reductions in large vessel flow velocity (Levine et al., 1994; Schondorf et al., 1997) and CBF in the distal part of the internal carotid artery domain (Hayashida et al., 1993; Ouchi et al., 2001a; Warkentin et al., 1992), occasionally along with a reduction in oxygen supply to the region (Mehagnoul-Schipper et al., 2000) during assumption of an upright posture. An orthostatic change of blood pressure may be a major contributor to cerebral ischemic stroke, because the magnitude of postural hypotension could be an index for cerebrovascular mortality rates (Raiha et al., 1995), and because reduced circadian blood pressure could trigger

* Corresponding author. Positron Medical Center, Hamamatsu Medical Center, 5000 Hirakuchi, Hamakita 434-0041, Japan. Fax: +81 53 585 0367.
E-mail address: ouchi@pmc.hmedc.or.jp (Y. Ouchi).
Available online on ScienceDirect (www.sciencedirect.com.)

1053-8119/$ - see front matter © 2004 Elsevier Inc. All rights reserved.
doi:10.1016/j.neuroimage.2004.07.044

further ischemic insults in poststroke patients (Lakka et al., 1999; Strandgaard and Paulson, 1989). Animal experiments have shown that when the systemic blood pressure decreases below the lower limit of cerebral autoregulation, multiple ischemic loci are generated (Hamar et al., 1979), and a reduction in the cerebral arteriolar pressure in the ischemic region distal to an arterial occlusion occurs (Paulson, 1970; Symon et al., 1976). The same theory could be applied to patients with internal carotid artery occlusive disease (ICAO), because there is a gradual decrease in regional cerebral blood flow (rCBF) together with an elevation in the oxygen extraction fraction (OEF) in an axial-direction fashion on the occlusion side (Yamauchi et al., 1990).

The purpose of the present study was to investigate, using positron emission tomography (PET), absolute changes in rCBF and oxygen metabolism in cerebrovascular patients with and without coronary artery disease during assumption of an upright posture in order to elucidate the orthostatic deterioration in hemodynamic and metabolic regulations in the hemodynamically vulnerable brain region.

Subjects and methods

Patients

The patient groups consisted of only patients with an occlusion or 99% stenosis in the unilateral ICA. Sixteen patients (11 men and 5 women) with cerebrovascular disease and 10 healthy volunteers (5 men and 5 women, 58.7 ± 6.7 years) participated. The patients were divided into two groups according to the comorbidity of clinically stable coronary artery disease (occlusion or stenosis); a group without cardiac problems (carotid artery occlusive disease (CVD) group; n = 10, 6 men and 4 women, mean ± SD, 65.1 ± 7.3 years) and a group with cardiac ischemia (coronary artery disease (CVDC) group; n = 6, 5 men and 1 woman, 64.2 ± 9.5 year). The third group (normal group) consisted of the 10 healthy volunteers. No significant difference was found in age among the three groups (t test, $P > 0.05$). The clinical characteristics of each patient are summarized in Table 1. Electrocardiogram showed a typical ST-segment depression in all CVDC patients and a small change of ST segment and T wave in

Table 1
Patient characteristics

No	Age	Sex	Diagnosis	Side	DD	Symptoms	Complications	HIAs on T2-MRI	AG	ECG	Medication
CVD											
1	53	M	ICAS	R	0.2	NS, Sensory disturbance	DM	subCx WM	BZ	normal	anti-DM
2	71	M	ICAO	L	0.5	R hemiparesis	None	L basal ganglia	BZ	normal	None
3	68	M	ICAS	R, L	0.4	L hemiparesis	HT	LR hemispheric subCx WM	PC	normal	anti-HT, anti-coag
4	57	M	ICAS	L, R	1.5	Tinnitus, TIA	HT	L frontal subCx WM	BZ	normal	anti-HT, anti-HMG
5	71	M	ICAO	R	0.3	Dysphagia, Dysphasia	None	LR hemispheric subCx WM	BZ	normal	anti-coag
6	72	M	ICAO	R	0.2	L weakness, impaired gait	None	R watershed subCx WM	BZ	normal	anti-coag
7	71	F	ICAO, ICAS	L, R	0.8	TIA (R motor weakness)	HT	L hemispheric subCx WM	PC	ST	anti-HT, anti-coag
8	69	F	ICAS	L	1.5	Mild apraxia	HT	R, L basal ganglia	CC, BZ	normal	anti-HT, anti-coag
9	56	F	ICAO	R	0.2	TIA (L motor weakness)	None	subCx WM	BZ	normal	anti-coag
10	63	F	ICAO	L	1.2	Tinnitus	None	subCx WM	BZ	normal	None
CVDC											
1	60	M	ICAOc	L	1.1	TIA (R motor weakness),	HT, HU, AP,	subCx WM	PC	ST	anti-HT, anti-AP, anti-HU
2	76	M	ICASc	L	0.4	Faintness, collapse,	MI, Ar	L hemispheric subCx WM	BZ	ST	anti-coag, anti-AP
3	53	M	ICASc	R	0.5	TIA (L motor weakness)	DM, AP	subCx WM	BZ	ST	anti-DM, anti-AP
4	55	F	ICAOc	L	0.3	Aphasia, TIA	HC, AP, Ar	L hemispheric subCx WM	PC	ST	anti-coag, anti-HC, anti-AP
5	72	M	ICAOc, ICASc	L, R	1.0	R, L hemiparesis	HT, AP	R, L subCx WM	BZ	ST	anti-HT, anti-AP
6	69	M	ICAOc	R	0.2	Dysartheia, Paraparesis	HT, AP	R, L subCx WM, pons	CC, BZ	ST	anti-HT, anti-AP

ICAO, internal carotid artery occlusion; ICAS, internal carotid artery stenosis; ICAOc, internal carotid artery occlusion with coronary artery disease; DD, disease duration from onset to PET measurement (years); TIA, transient ischemic attack; HIAs, high intensity areas; ECG, electrocardiogram; ST, ST-segment depression and T wave changes; Cx, cortex; subCx, subcortex; WM, white matter; AG, angiography; BZ, border zone shift; CC, cross circulation; PC, pial collateralization to the insula level; HT, hypertension; DM, diabetes mellitus; HU, hyperuricemia; AP, angina pectoris; MI, myocardial infarction; HC, hypercholesteremia; Ar, arrhythmia; R, right; L, left; anti-HT, anti-hypertensive drug; anti-HMG, 3-hydroxy-3methylglutaryl-coenzyme A (HMG-CoA) reductase inhibitor for treatment of hypercholesterolemia; anti-DM, oral drug for Diabetes mellitus; anti-coag, anticoagulant drug.

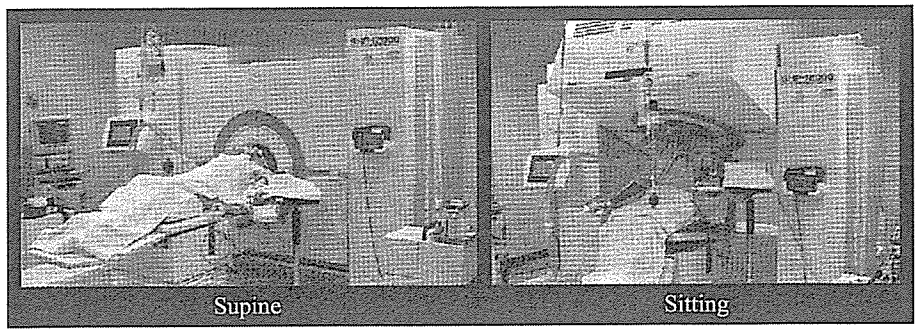

Fig. 1. The scene of PET measurements during the supine and sitting conditions.

one CVD patient. Angiographic studies revealed the cross circulation through the circle of Willis, leptomeningeal collateralization, and the border zone shift according to the definition of the St Louis group (Derdeyn et al., 1999) in all 16 patients, and coronary artery branch stenosis or occlusion in all six CVDC patients (see Table 1). The border zone shift includes the asymmetry filling of anterior or posterior cerebral artery that feeds the middle cerebral artery on the compromised side. The leptomeningeal flow in the parietal region was occasionally seen in the case of retrograde filling from the posterior cerebral artery circulation. Specifically, all the CVDC patients revealed a degree of leptomeningeal connections at the level of posterior watershed regions (middle cerebral artery and posterior cerebral artery border zone). In the two patient groups, none of the patients reported orthostatic symptoms during PET measurement. All of the patients were receiving treatment with antihypertensives, anticoagulants, and other conventional drugs for complications (see Table 1), treatment that could not be suspended before the PET scans were conducted. However, all of these medications were temporarily suspended on the day of the PET examinations. All of the patients underwent magnetic resonance imaging (MRI), which showed mild-to-moderate subcortical abnormalities (high intensities on the T2-weighted images) in the territory of the ICA on the occluded side and no involvement of the lobe infarction. The study protocol was approved by the Ethics Committee of the Hamamatsu Medical Center, and all participants gave their written informed consent after the nature and possible risks of the experiment were explained.

Postural condition and physiology

First, each participant lay calmly with his/her eyes closed on the scanner couch for approximately 40 min. After the supine condition examination was completed, the subjects were instructed to sit back against a 65° reclined (chair-like) couch with their eyes closed for about 25 min (Fig. 1). In both conditions, we recorded systemic arterial blood pressure (ABP) via a catheter placed in the brachial artery and the cardiac rhythm by electrocardiogram. Other physiological parameters, such as PaO_2, $PaCO_2$, and pH, were measured periodically. In our preliminary study, a very short-term elevation of systemic ABP after a postural shift from the supine to the sitting position was found, followed by a gradual decline to the plateau level within about 3 min. These findings were in agreement with results from

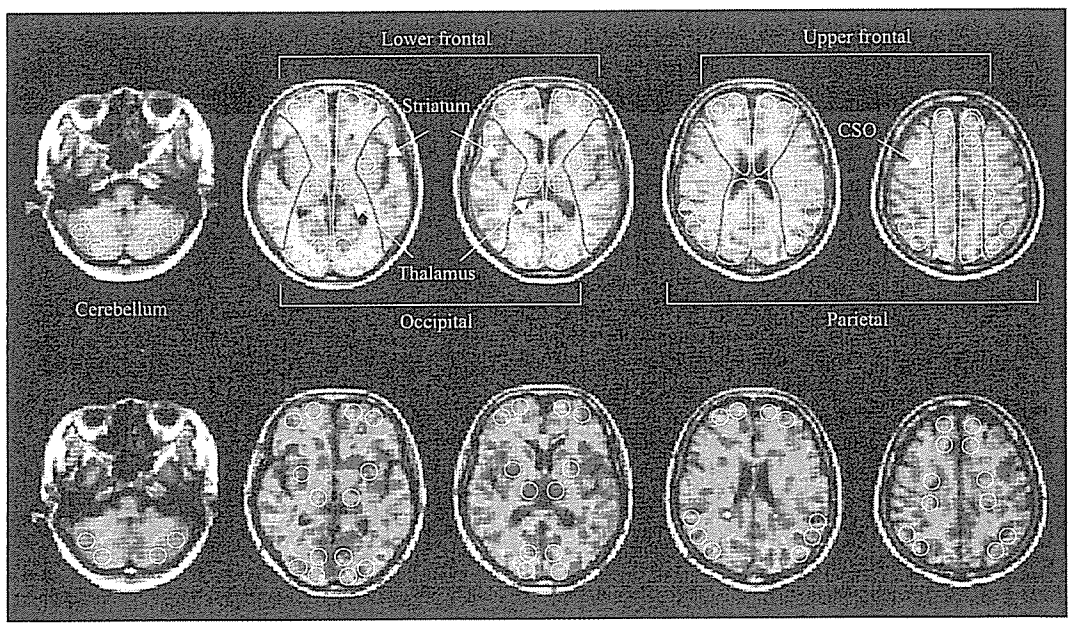

Fig. 2. ROI setting. Multiple circular ROIs consisting of 96 pixels (1.58 cm^2) were placed on the brain regions on the reformatted MR images (upper row) with the same pixel size as that of PET, which were automatically transferred onto the PET images (lower row). CSO, centrum semiovale.

a previous ultrasonic study (Novak et al., 1998). Thus, the orthostatic PET measurements in this study were performed during the static period of ABP under the head-up condition.

PET and MRI procedures

We used a state-of-the-art high-resolution brain PET scanner (SHR12000, Hamamatsu Photonics, Hamakita, Japan), the details of which have been reported elsewhere (Watanabe et al., 2002). In brief, the scanner has 24 detector rings yielding 47 slices simultaneously with a spatial resolution of 2.9 mm (full-width at half-maximum) transaxially and 3.0 mm axially and 163 mm axial field of view. After the backprojection and filtering (Hanning filter), the reconstructed image resolution became 6.0 × 6.0 × 3.2 mm full-width at half-maximum. The voxel of each reconstructed image measured 1.3 × 1.3 × 3.2 mm. This PET system has a mobile gantry system in which the gantry can move vertically 180 cm above the floor and tilt from −20° to +90° like a mechanical chair. Just prior to the PET measurements, each participant underwent an MRI for determination of the intercommissural (AC-PC) line using a static magnet with three-dimensional mode acquisition (0.3 T MRP7000AD, Hitachi, Japan) (Ouchi et al., 1998). Because the same face mask was used between the MRI and PET studies, and because the center of scan field was beforehand calibrated between the two modalities, the PET gantry was moved, and the brain was scanned parallel to the intercommissural plane according to the MRI information received.

After fixation of the head to the head holder using a radiosurgery-purpose thermoplastic face mask, a 10-min transmission scan was first performed for attenuation correction with a $^{68}Ge/^{68}Ga$ source in the supine position. Then the serial emission scans were started based on ^{15}O-oxygen bolus inhalation (Mintun et al., 1984) and ^{15}O-water bolus injection method (Herscovitch et al., 1983) and short-period $C^{15}O$ inhalation for the cerebral blood volume (CBV) data (Lammertsma and Jones, 1983; Lammertsma et al., 1987). During the scan session, the subjects inhaled 2.0 GBq $^{15}O_2$ and, for a short period of time, 1500 MBq $C^{15}O$ flowing through a tightly fitted plastic oxygen face mask attached to the subject's face. They also received 300 MBq $H_2^{15}O$ via a catheter in the right cubital vein. Data of arterial oxygen saturation (SaO_2), arterial hemoglobin (Hb), and the hematocrit values yielded the arterial oxygen content (CaO_2) by the following formula: $CaO_2 = 1.39 \times SaO_2 \times Hb$. The rCBF- and CBV-corrected OEF values were estimated on a voxel-by-voxel basis. The voxel-based $CMRO_2$ image was finally generated using the following equation: $CMRO_2 = CBF \times OEF \times CaO_2$. The arterial blood radioactivity was determined using the automated arterial blood γ-ray coincidence counter (BACC-2: Hamamatsu Photonics K.K.), which could measure arterial input data per second (Ouchi et al., 2001b). After the first session of PET scans under the supine condition was completed, the subject's head holder was temporarily removed from the receiver of the scanner's gantry, and the head was fixated again in the sitting position. Emission scans with the same protocol were performed under the sitting condition.

Data analysis and statistics

As seen in Fig. 2, we first placed multiple circular regions of interest (ROIs) with 96 pixels (1.62 cm^2) bilaterally over the cerebellar hemisphere, lower frontal area (the orbitofrontal and inferior frontal cortices [Brodmann area or BA: 10/11]), upper frontal area (middle and superior frontal cortices [BA: 6/8]), temporal [BA: 21/22], parietal [BA: 7], occipital [BA: 17/18] cortices, the striatum, the thalamus, and the centrum semiovale (CSO) on the MR images according to the human brain atlas (Mai et al., 1997; Ouchi et al., 2001b). After completion of the ROI placement, the PET images were displayed side-by-side with the MR images using an image processing system (DrView, Asahi Kasei Co, Tokyo, Japan) (Ouchi et al., 2001a,b) on a SUN workstation (Hypersparc ss-20, SUN Microsystems, CA, USA), which enabled the automatic placement of ROIs on the same area on both the MR and corresponding PET images (CBF, $CMRO_2$, OEF, CBV under both supine and sitting conditions). Quantitative data in the normal group were calculated by averaging the bilateral values in each region. The ROIs on the upper frontal and parietal region as well as the CSO were regarded as the loci for the distal part of the affected ICA territory.

For statistical analysis, baseline data collected in the supine posture were compared among the three groups by two-way analysis of variance (ANOVA) with respect to the type of group (CVD, CVDC, and Normal) and type of location, that is, occluded or non-occluded side. Since no cross-interactions were observed in the ANOVA between the two factors ($P = 0.4384$), repeated measure ANOVA was then performed to compare the parameters among groups on each hemispheric side separately. Since the perfusion territorial changes in hemodynamic param-

Table 2
Physiological data in patients with cerebrovascular disease and normal controls

Group	Condition	MABP	Pulse rate	$PaCO_2$	pH
CVD	Supine	103.2 ± 11.3*	72.3 ± 14.3	40.3 ± 3.4	7.4 ± 0.0
	Sitting	99.5 ± 14.7*	74.3 ± 14.9	40.2 ± 3.4	7.4 ± 0.0
	Change (%)	−3.36	3.10	−0.72	0.0
CVDC	Supine	95.7 ± 8.9	73.2 ± 11.6	41.1 ± 2.0	7.4 ± 0.0
	Sitting	90.8 ± 8.2	74.5 ± 8.5	40.6 ± 1.9	7.4 ± 0.0
	Change (%)	−5.1	2.5	−1.1	−0.1
NC	Supine	94.0 ± 8.0	62.4 ± 7.3	41.7 ± 2.9	7.4 ± 0.0
	Sitting	91.2 ± 8.1	65.9 ± 6.8	41.8 ± 3.5	7.4 ± 0.0
	Change (%)	−2.93	3.49	0.01	0.0

Values are expressed as mean ± SD. CVD, cerebrovascular disease (internal carotid artery occlusion or severe stenosis); CVDC, CVD with coronary artery disease; NC, normal controls; MABP, mean arterial blood pressure; Change (%), ([sitting − supine]/supine × 100) expressed as a mean value.
* $P < 0.05$ (χ^2 test) vs. normal control.

Table 3
Parameter changes by postural shift in patients with cerebrovascular disease and normal controls

Group	Parameter	State	Cerebellum		Lower frontal		Upper frontal		Parietal		Occipital		Striatum		Thalamus		CSO	
			Intact	Affected	Intact	Affected	Intact	Affected	Intact	Affected	Intact	Affected	Intact	Affected	Intact	Affected	Intact	Affected
CVD	CBF	Supine	42.6 ± 8.8	47.9 ± 9.7	40.2 ± 4.7	35.3*** ± 8.4	43.8 ± 7.0	39.3*** ± 8.7	41.5 ± 8.3	38.7*** ± 8.7	41.7 ± 9.2	41.8 ± 9.9	51.8 ± 9.9	43.8 ± 10.9	52.5 ± 10.4	48.2 ± 9.8	24.0 ± 4.5	23.9 ± 4.8
		Sitting	41.0 ± 7.9	46.8 ± 8.1	39.2 ± 6.0	34.0 ± 8.9	42.2 ± 5.6	36.6 ± 8.0	40.2 ± 8.3	35.6 ± 8.0	40.0 ± 8.7	40.1 ± 6.2	45.7 ± 9.1	36.2 ± 9.3	49.0 ± 10.1	44.8 ± 9.3	23.6 ± 4.6	22.2 ± 5.6
		%Δ	−3.28	−3.04	−3.1	−3.6	−3.48	−5.89	−2.75	−6.59***	−1.76	−1.62	−2.50	−5.12	−4.85	−6.39	−2.67	−4.83
	$CMRO_2$	Supine	3.1 ± 0.8	3.4 ± 0.9	2.7 ± 0.7	2.6 ± 0.8	3.0 ± 0.6	3.0 ± 0.7	2.7 ± 0.8	2.9 ± 0.8	2.8 ± 1.2	2.8 ± 1.1	3.3 ± 1.0	3.1 ± 1.1	3.2 ± 0.7	3.0 ± 1.2	1.1 ± 0.5	1.2 ± 0.6
		Sitting	3.3 ± 1.0	3.3 ± 0.8	2.7 ± 0.9	2.6 ± 0.8	2.6 ± 0.8	2.7 ± 0.8	2.8 ± 0.9	2.8 ± 1.0	3.1 ± 0.9	2.9 ± 1.0	2.7 ± 1.1	2.6 ± 1.0	3.0 ± 1.0	3.8 ± 1.2	1.4 ± 0.7	1.3 ± 0.6
		%Δ	3.45	2.71	2.02	2.2	3.94	3.18	5.22	2.88	3.33	4.32	−0.20	−0.26	1.12	−0.72	2.18	1.77
	OEF	Supine	39.9 ± 7.0	40.4 ± 7.8	42.0 ± 7.0	42.8*** ± 8.2	40.3 ± 5.1	40.9 ± 5.2	40.9 ± 6.1	42.4*** ± 5.6	42.6 ± 8.0	42.8 ± 8.8	40.0 ± 8.4	39.1 ± 8.4	37.2 ± 7.7	37.8 ± 8.1	32.4 ± 7.3	34.3 ± 6.2
		Sitting	43.0 ± 10.2	41.4 ± 8.4	43.1 ± 9.5	44.4 ± 9.0	41.5 ± 7.8	44.7 ± 7.2	44.1 ± 6.5	48.6 ± 7.8	43.8 ± 9.0	45.1 ± 8.7	40.3 ± 9.3	40.5 ± 9.3	38.5 ± 10.4	40.0 ± 9.8	33.0 ± 6.8	35.8 ± 5.3
		%Δ	5.06	4.74	4.10	6.22	6.97	10.81***	8.9	16.09**	4.10	6.22	4.53	5.06	4.74	6.98	7.90	6.08
	CBV	Supine	3.8 ± 0.5	4.3 ± 1.0	2.9 ± 0.5	3.0 ± 0.7	2.7 ± 0.6	2.6 ± 0.3	3.2 ± 0.7	3.6 ± 0.9	3.6 ± 0.5	4.3 ± 1.0	2.7 ± 0.4	2.6 ± 0.3	2.4 ± 0.6	3.0 ± 0.6	1.9 ± 0.4	1.9 ± 0.5
		Sitting	3.8 ± 0.8	4.7 ± 1.8	3.0 ± 0.5	3.1 ± 0.6	3.0 ± 0.3	2.8 ± 0.4	3.2 ± 0.7	3.6 ± 0.6	3.7 ± 0.4	4.1 ± 0.6	2.7 ± 0.3	2.6 ± 0.3	2.3 ± 0.3	3.9 ± 0.7	2.0 ± 0.7	1.8 ± 0.4
		%Δ	−0.55	3.01	4.78	2.39	5.8	5.08	3.52	0.78	4.52	4.13	−2.86	2.17	−0.54	3.12	0.87	0.29
CVDC	CBF	Supine	38.2 ± 0.8	42.3 ± 12.3	34.0 ± 11.0	32.5*** ± 6.1	35.5 ± 10.8	34.6 ± 9.7	35.9 ± 8.5	31.4*** ± 8.2	33.3 ± 8.4	29.9*** ± 10.4	44.9 ± 16.6	45.1 ± 12.1	43.5 ± 16.2	40.2 ± 13.5	18.3 ± 5.6	20.1 ± 6.4
		Sitting	35.4 ± 12.2	37.0 ± 11.5	33.0 ± 10.3	31.5 ± 7.3	32.2 ± 9.9	29.2 ± 7.2	31.9 ± 7.9	26.8 ± 7.7	34.0 ± 9.2	29.5 ± 9.0	39.3 ± 15.1	37.4 ± 12.7	43.6 ± 11.4	40.1 ± 10.4	18.0 ± 5.4	16.8 ± 6.7
		%Δ	−8.6	−10.5	−4.3	−3.4	−10.4	−14.7***	−12.2	−14.1*,**	−9.2	−10.3	−12.5	−15.7***	−1.6	−0.3	−1.9	−4.1
	$CMRO_2$	Supine	2.6 ± 0.6	2.6 ± 0.7	2.4 ± 0.8	2.3 ± 0.5	2.4 ± 0.6	2.3 ± 0.5	2.4 ± 0.6	1.9** ± 0.8	2.4 ± 0.5	2.1 ± 0.9	3.2 ± 1.2	3.0 ± 0.6	2.7 ± 0.7	2.8 ± 1.1	1.1 ± 0.4	1.1 ± 0.5
		Sitting	2.8 ± 0.9	2.6 ± 0.8	2.4 ± 1.1	2.3 ± 0.5	2.3 ± 0.9	2.2 ± 0.6	2.5 ± 0.7	1.9 ± 0.9	2.3 ± 0.7	2.1 ± 1.0	2.9 ± 1.2	3.0 ± 0.5	2.7 ± 1.0	2.8 ± 1.3	0.9 ± 0.2	1.2 ± 0.6
		%Δ	7.2	1.2	−1.2	0.6	−4.4	−5.2	5.2	−7.8*,**	−5.7	−2.1	−9.3	0.1	−2.2	−1.0	−9.8	6.8
	OEF	Supine	43.1 ± 5.1	38.6 ± 5.8	42.0 ± 7.9	42.9 ± 8.1	39.3 ± 8.5	40.7 ± 9.2	40.8 ± 6.3	40.3 ± 3.5	41.6 ± 9.3	38.3 ± 10.2	43.5 ± 5.6	38.2 ± 6.1	35.4 ± 9.3	36.3 ± 7.8	28.3 ± 5.7	26.5 ± 9.0
		Sitting	46.4 ± 7.7	41.8 ± 4.0	44.4 ± 2.8	43.8 ± 6.7	42.0 ± 8.1	46.0 ± 8.6	43.5 ±	45.2 ± 3.7	46.5 ± 9.6	38.0 ± 11.2	41.4 ± 5.9	44.6 ± 8.7	31.9 ± 8.4	37.3 ± 6.9	28.0 ± 4.1	28.8 ± 8.1
		%Δ	7.4	9.2	6.6	3.5	7.7	14.1***	6.0	12.8***	11.7	6.4	−4.8	16.6	−9.0	3.5	0.1	11.3
	CBV	Supine	4.0 ± 0.8	4.5 ± 0.7	3.9 ± 4.0	3.6 ± 1.9	3.1 ± 0.6	3.1 ± 0.7	3.4 ± 0.5	3.9 ± 0.8	3.8 ± 0.6	4.5 ± 2.1	3.3 ± 1.4	3.4 ± 1.2	3.6 ± 0.8	3.0 ± 0.3	2.2 ± 0.4	2.7 ± 0.9
		Sitting	4.1 ± 0.7	4.5 ± 0.8	3.5 ± 0.7	3.5 ± 0.8	2.9 ± 0.3	3.0 ± 0.5	3.5 ± 0.6	3.5 ± 0.6	4.0 ± 0.7	4.2 ± 1.9	2.9 ± 0.7	3.2 ± 1.2	3.6 ± 0.7	3.2 ± 0.2	2.3 ± 0.6	2.5 ± 0.9
		%Δ	5.8	4.8	−10.6	−3.5	−2.2	−2.7	3.8	−4.8	5.2	−2.1	−5.9	−7.0	0.2	6.4	−1.3	−6.9
Normal	CBF	%Δ	−2.6		−4.43		−4.87		−4.92		−4.59		−5.43		−5.41		−2.58	
	$CMRO_2$	%Δ	1.51		−2.11		2.05		0.45		0.01		−0.21		−0.38		1.61	
	OEF	%Δ	3.7		5.36		5.9		5.61		5.8		5.38		5.2		5.49	
	CBV	%Δ	−1.34		3.29		1.14		4.87		4.23		−1.64		4.51		1.25	

Values are expressed as %. CVD, cerebrovascular patients (internal carotid artery occlusive disease); CVDC, internal carotid artery occlusive disease with coronary artery disease; NC, normal controls; CSO, centrum semiovale; CBF, cerebral blood flow; $CMRO_2$, cerebral metabolic rate of oxygen; OEF, oxygen extraction fraction; CBV, cerebral blood volume; %Δ: ([sitting − supine]/supine × 100).

* $P < 0.05$ vs. CVD.

** $P < 0.05$ vs. normal controls.

*** $P < 0.1$ (subsignificant) vs. normal controls.

eters (i.e., the ICA territory) were of interest, a Bonferroni post hoc test was applied within the same territory, and a P value less than 0.05 was regarded as statistically significant. Simple linear regression analyses were performed to analyze the relation between postural changes of metabolic parameters ($CMRO_2$ and OEF) and the changes of the perfusion pressure index (CBF/CBV) in the CVD and CVDC groups, separately. In addition, the postural changes in these hemodynamic parameters were compared against the changes in mean ABP in the distal ICA regions. The level of significance was also assumed as $P < 0.05$.

In addition, we added a voxel-based analysis to evaluate postural changes in rCBF more objectively between disease and healthy conditions using statistical parametric mapping (SPM) software (SPM99; Wellcome Department of Cognitive Neurology, London, UK) (Friston et al., 1995). The detail procedure was reported elsewhere (Ouchi et al., 2001a). In brief, normalized data were smoothed with an isotropic Gaussian kernel of 8 mm, resulting in the smoothed images with voxel sized of $2 \times 2 \times 2$ mm. In the present study, however, we used quantitative CBF data for the voxel-wise analysis without analysis of covariance with global normalization. The regions with clusters of voxels over 50 and a peak height $P < 0.001$ uncorrected for multiple comparison were regarded as significant. In addition, a single-subject analysis was performed to examine individual variability. The significant level of this analysis was assumed to be $P < 0.003$ uncorrected for multiple comparison for the peak height with voxels over 50.

Results

Physiological changes

There was a tendency for postural decrease of the mean arterial blood pressure (MABP) in the CVDC group to occur, but the physiological parameters (MABP, pulse rate, $PaCO_2$, and arterial pH) were not significantly different between the supine and upright conditions among the three groups ($P > 0.05$, repeated-measures ANOVA) (Table 2). No clinical symptoms, such as hyperventilation, faintness, and syncope, were observed during the upright posture in any of the participants. Each electrocardiogram showed no significant ST-segment depression during the upright condition in the CVDC group.

ANOVA for absolute postural changes in hemodynamic and metabolic parameters

At baseline, one-way ANOVA showed significant reductions in rCBF in the parietal, frontal, and occipital cortices on the affected side and in the $rCMRO_2$ in the parietal counterpart in the CVDC group compared with the normal group ($P < 0.05$, Table 3). Repeated measures ANOVA showed significant absolute reductions in rCBF and $rCMRO_2$ in the affected-side parietal cortex in the CVDC group during upright posture compared with those in the CVD and normal groups, while rCBF (with a decrease tendency) and the $rCMRO_2$ in the area failed to show significant changes in the CVD group. The level of OEF in the affected-sided parietal cortex during sitting was significantly higher in the disease groups than that in the normal group (similar to the hemodynamic change "misery perfusion") (Baron et al., 1981). Table 4 showed mean levels of each parameter estimated for values of the territory of ICA, hemispheric, and global regions.

Relations between postural changes in oxygen metabolic parameters ($CMRO_2$, OEF) and changes in perfusion pressure index (CBF/CBV)

There were significant negative correlations of the postural changes in %ΔCBF/CBV with %ΔOEF in the upper frontal ($y = -1.38x - 6.12$, $r = 0.70$, $P < 0.05$) and parietal ($y = -1.03x - 1.73$, $r = 0.79$, $P < 0.05$) cortices and with %Δ$CMRO_2$ in the upper frontal ($y = -1.59x - 28.5$, $r = 0.68$, $P < 0.05$) and parietal ($y = -1.97x - 32.3$, $r = 0.73$, $P < 0.05$) cortices on the affected side in the CVDC group (Fig. 3), indicating that metabolic demand was raised as perfusion pressure decreased. In the CVD group, the postural changes in the parietal OEF tended to correlate negatively with the CBF/CBV changes ($r = 0.59$, dotted line) on the affected side, while the two parameters showed positive correlation ($r = 0.57$, dotted line) on the non-occluded side (Fig. 3D).

Relations between postural changes in hemodynamic and metabolic parameters and mean arterial blood pressure

Because the parameters varied significantly in the parietal cortex, we focused on changes in this region. In other brain regions, there was a similar tendency in the upper frontal cortex (not shown).

Table 4
Mean levels of territorial cerebral blood flow during the postural conditions (supine/sitting) in three groups

Group	Parameter	Global	Hemisphere		ICA territory	
			Intact	Affected	Intact	Affected
CVD	CBF	42.9/41.4	46.6/45.2	42.6/40.4	45.7/44.1	41.2/39.1
	CMRO	2.8/2.9	3.1/3.1	2.9/2.9	3.0/3.1	2.8/2.9
	OEF	38.9/41.0	39.4/41.3	39.8/42.5	39.6/41.8	40.2/43.3
	CBF/CBV	13.6/13.0	14.9/14.4	13.8/12.8	15.0/14.3	13.4/12.4
CVDC	CBF	35.9/33.5	37.9/36.2	35.8/33.1	35.9/34.4	34.3/31.7
	CMRO	2.33/2.41	2.6/2.6	2.4/2.4	2.4/2.5	2.3/2.2
	OEF	37.4/39.9	39.2/40.7	38.5 41.5	38.6/41.2	41.1/43.4
	CBF/CBV	10.7/10.1	11.5/10.9	10.8/10.0	10.5/10.4	10.4/9.9
NC	CBF	43.8/42.1	46.9/44.4	46.4/44.8	43.4/42.0	43.5/41.7
	CMRO	2.7/2.7	2.9/2.9	2.8/2.8	2.7/2.7	2.7/2.7
	OEF	43.8/42.2	38.6/40.4	37.0/38.3	38.7/40.0	38.0/39.4
	CBF/CBV	12.8/12.0	13.6/12.4	13.1/12.4	12.8/11.9	13.0/12.3

CBF, cerebral blood flow (ml/100 g/min); $CMRO_2$, cerebral metabolic rate of oxygen (ml/100 g/min); OEF, oxygen extraction fraction (%); CBV, cerebral blood volume (ml/100 g), CBF/CBV (%).

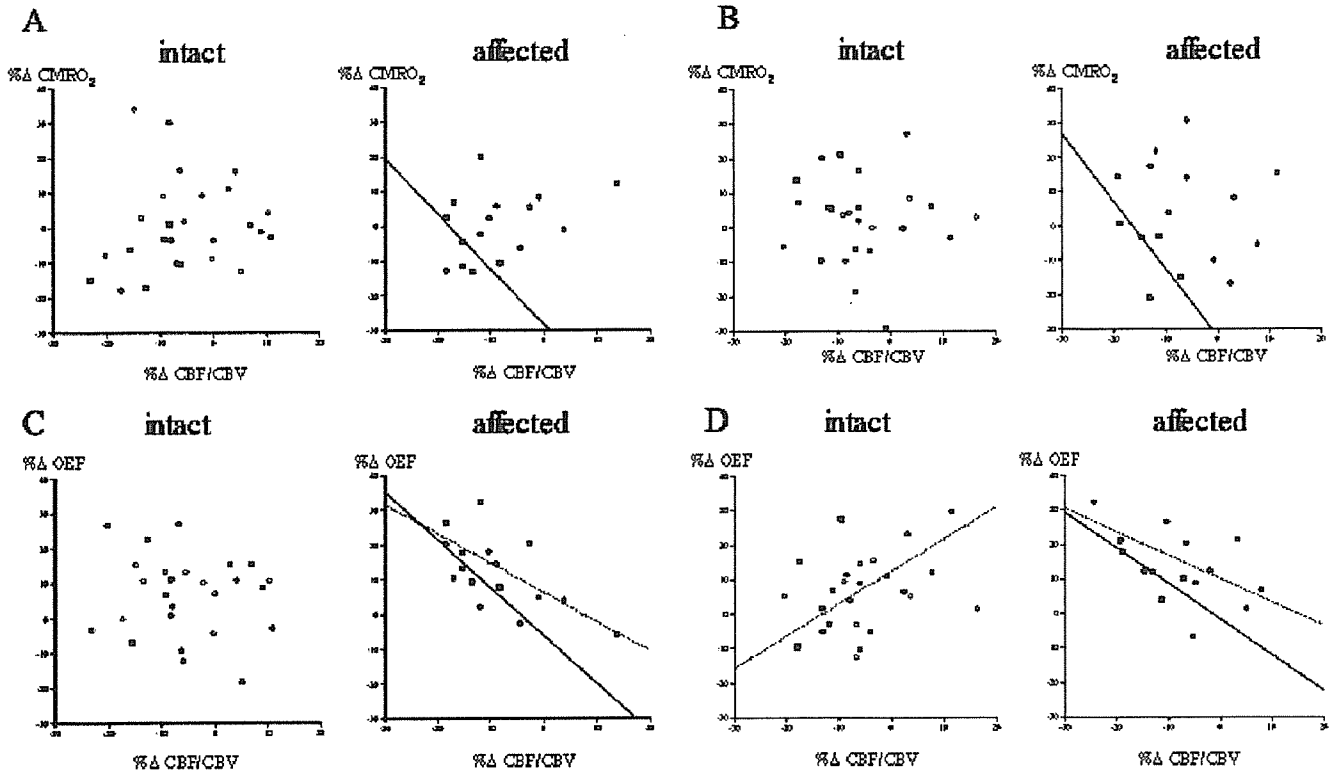

Fig. 3. Correlations between changes in perfusion pressure index (CBF/CBV) and changes in oxygen metabolism (A and B) and oxygen extraction fraction (C and D) in susceptible regions (A and C, upper frontal cortex; B and D, parietal cortex) in the normal (white circle), CVD (black circle, dotted line), and CVDC (marked square, straight line) groups. Straight lines denote significant correlations ($P < 0.05$), and dotted lines show subsignificant correlations ($P < 0.1$).

In the normal group, the values of CBF, $CMRO_2$, and OEF in the parietal cortex were almost constant with the MABP change (Figs. 4A–C, intact side, dashes). However, postural reduction in rCBF became significantly greater with MABP reduction ($y = 2.82x + 0.22$, $r = 0.80$, $P < 0.05$) in the CVDC group (Fig. 4A, affected side). Postural changes in metabolic parameters (OEF) significantly correlated negatively with MABP change ($y = -4.03x - 7.63$, $r = 0.88$, $P < 0.05$) (Fig. 4C, affected side), and so did the $CMRO_2$ change ($y = -7.07x - 40.5$, $r = 0.74$, $P < 0.05$) (Fig. 4B, affected side). In the CVD group, the rCBF change tended to correlate positively ($r = 0.60$, Fig. 4A, affected side) and the OEF change negatively ($r = 0.50$, Fig. 4C, affected side) with the MABP change.

Discussion

The present study is the first to show an absolute reduction in CBF and an increase in OEF along with a minor increase in oxygen metabolism in the hemodynamically compromised parietal region (i.e., the region more distal to the occlusion and comparable to the watershed area) in CVD patients during upright posture, suggesting the occurrence of posture-induced local neural tissue deactivation, and a further reduction in rCBF and a moderate increase in OEF along with reduced oxygen metabolism (severer deactivation) in the CVDC patients during posture (Figs. 5 and 6). Although the levels of CBV were not significantly different between postural conditions in each group, the averaged CBV values in the CVDC group tended to decrease during upright posture. The major difference between the CVD and CVDC groups was the opposite deviation in $CMRO_2$ changes in the ischemic region by a postural shift. A postural increase in OEF was commonly found in both groups, but the magnitude of the OEF increase was smaller in the CVDC group, which might cause postural reduction in $CMRO_2$. The lack of this capacity to maintain $CMRO_2$ in the CVDC group may be attributable to neuronal impairment or the scantiness of the available vascular density. It has been hypothesized that in patients with coronary artery disease, reduced flow, microemboli, and small necrosis are likely to develop due to a physical and mental stress-induced increase in blood viscosity and coagulability (Muller et al., 1989). This insidious damage in the susceptible cerebrovasculature would prevent augmentation of oxygen metabolism in the CVDC group. A greater reduction in perfusion pressure (CBF/CBV) in CVDC patients than in CVD patients might have been another explanation for the loss of metabolic increase. Taken together, upright posture may generate not only local neural deactivation in the distal part of the brain in the occluded ICA territory, but also impairment of local metabolic regulation in the area, if concomitant with cardiac ischemia. The latter problem can be a consecutive setback in the recovery of neuronal function during rehabilitation.

The postural effect on cerebral hemodynamics has been widely examined with transcranial Doppler sonography that enables the assessment of orthostatically rapid hemodynamic changes. The greater advantage of our study over sonography was the ability to quantitatively measure not only vascular, but also metabolic states in cerebrovascular regulations during assumption of the upright posture. An absolute reduction in rCBF in the hemodynamically vulnerable region under our orthostatic conditions was in line with the sonographic result showing orthostatic reduction in the perfusion velocity of intracranial large vessels (Fig. 7; Daffertshofer et al., 1991; Novak et al., 1998). As for methodological

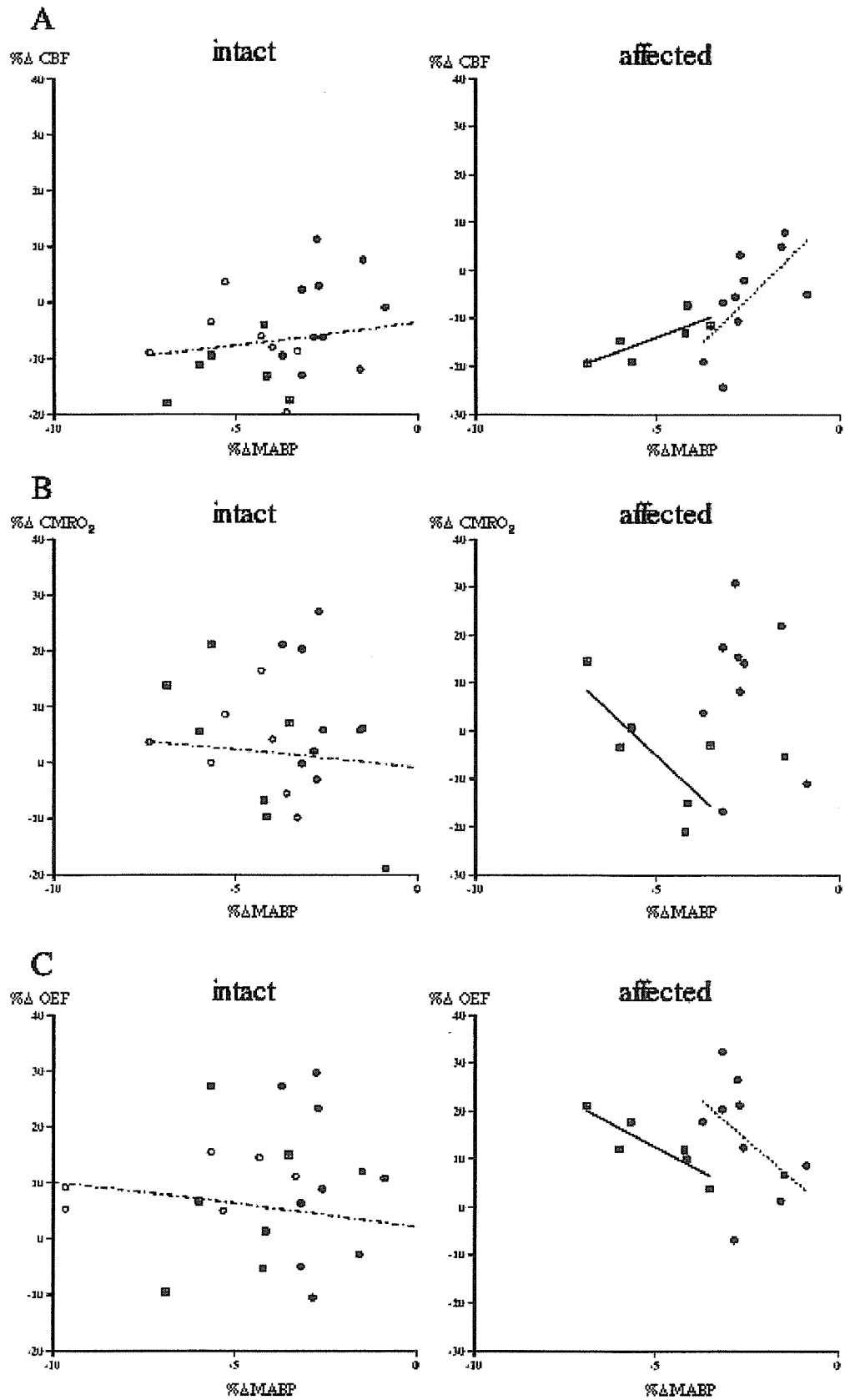

Fig. 4. Correlations of %reduction in mean arterial blood pressure (%ΔMABP) with %changes in perfusion (%ΔCBF, A), oxygen metabolism (%ΔCMRO$_2$, B), and oxygen demand index (%ΔOEF, C) in the hemodynamically vulnerable parietal region in the normal (white circle, dashes), CVD (black circle, dotted line) and CVDC (marked square, straight line) groups. While the cerebrovascular and metabolic parameters reached a plateau with the MABP change in the normal group, significant correlations were observed in the disease groups (see the Results), although the width of the MABP change was relatively small.